Hearing Research 341 (2016) 50–65

Contents lists available at ScienceDirect

Hearing Research

journal homepage: www.elsevier.com/locate/heares

Research paper

Across-site patterns of electrically evoked compound action potential amplitude-growth functions in multichannel cochlear implant recipients and the effects of the interphase gap

Kara C. Schvartz-Leyzac [a, b, *], Bryan E. Pfingst [a]

[a] Kresge Hearing Research Institute, Department of Otolaryngology, University of Michigan Health Systems, 1150 West Medical Center Drive, Ann Arbor, MI 48109-5616, USA

[b] Hearing Rehabilitation Center, Department of Otolaryngology, University of Michigan Health Systems, 475 W. Market Place, Building 1, Suite A, Ann Arbor, MI 48108, USA

ARTICLE INFO

Article history:
Received 6 May 2016
Received in revised form
1 August 2016
Accepted 9 August 2016
Available online 10 August 2016

Keywords:
Cochlear implant
Electrically evoked compound action potential
Electrode-neural interface

ABSTRACT

Electrically evoked compound action potential (ECAP) measures of peak amplitude, and amplitude-growth function (AGF) slope have been shown to reflect characteristics of cochlear health (primarily spiral ganglion density) in anesthetized cochlear-implanted guinea pigs. Likewise, the effect of increasing the interphase gap (IPG) in each of these measures also reflects SGN density in the implanted guinea pig. Based on these findings, we hypothesize that suprathreshold ECAP measures, and also how they change as the IPG is increased, have the potential to be clinically applicable in human subjects. However, further work is first needed in order to determine the characteristics of these measures in humans who use cochlear implants.

The current study examined across-site patterns of suprathreshold ECAP measures in 10 bilaterally-implanted, adult cochlear implant users. Results showed that both peak amplitude and slope of the AGF varied significantly from electrode to electrode in ear-specific patterns across the subjects' electrode arrays. As expected, increasing the IPG on average increased the peak amplitude and slope. Across ears, there was a significant, negative correlation between the slope of the ECAP AGF and the duration of hearing loss. Across-site patterns of ECAP peak amplitude and AGF slopes were also compared with common ground impedance values and significant correlations were observed in some cases, depending on the subject and condition. The results of this study, coupled with previous studies in animals, suggest that it is feasible to measure the change in suprathreshold ECAP measures as the IPG increases on most electrodes. Further work is needed to investigate the relationship between these measures and cochlear implant outcomes, and determine how these measures might be used when programming a cochlear-implant processor.

Published by Elsevier B.V.

1. Introduction

Several factors have been shown to contribute to speech understanding outcomes in cochlear implant (CI) recipients (Holden et al., 2013). It is often observed in the clinic that patients with a longer duration of deafness perform poorer with CIs compared to recipients with a shorter duration of deafness. Prolonged duration of deafness is associated with degeneration of cochlear structures (Nadol, 1997). This suggests that cochlear health (e.g., number of surviving hair cells, spiral ganglion neuron (SGN) density and myelination, among other factors) should vary across subjects and might help to explain the variability reported in speech recognition outcomes. Therefore, it seems reasonable that neural populations could be targeted for interventions either through programming adjustments (Garadat et al., 2013; Zhou and Pfingst, 2014) or neurotrophin gene therapy (Pfingst et al., 2014) in order to improve performance with an implant. Evidence to date using post-mortem

Abbreviations: ECAP, electrically evoked compound action potential; IPG, interphase gap; AGF, amplitude-growth function; CI, cochlear implant; SGN, spiral ganglion neuron; EABR, electrically evoked auditory brainstem response; ASM, Across-site mean

* Corresponding author. Kresge Hearing Research Institute, Department of Otolaryngology, University of Michigan Health Systems, 1150 West Medical Center Drive, Ann Arbor, MI 48109-5616, USA.

E-mail addresses: kleyzac@med.umich.edu (K.C. Schvartz-Leyzac), bpfingst@umich.edu (B.E. Pfingst).

http://dx.doi.org/10.1016/j.heares.2016.08.002
0378-5955/Published by Elsevier B.V.

temporal bone analyses has not supported the idea that neural density is related to speech recognition performance examined across subjects (Nadol et al., 2001; Khan et al., 2005). However, a more recent study using bilaterally-implanted subjects provides some evidence that within-subject differences in SGN density across ears did relate to within-subject speech recognition abilities across ears (Seyyedi et al., 2014). There are issues, however, when comparing post-mortem studies with speech recognition primarily concerning the long duration of time that occurs between points at which speech recognition measures are obtained and the point at which temporal bones are harvested for processing.

Here, we propose that the electrically evoked compound action potential (ECAP) may be a better tool to estimate neural density in human cochlear implant recipients because the ECAP data can be obtained during the same time period as other functional measures such as speech recognition. Data obtained in the implanted guinea pig suggest that good estimates of SGN density can be obtained during life using ECAP measures (Prado-Guitierrez et al., 2006; Ramekers et al., 2014; Pfingst et al., 2015). These studies reported a significant relationship between SGN density and suprathreshold measures of the ECAP when measured in cochlear-implanted guinea pigs, accounting for 50% of the variance or more in SGN density. Of particular interest in the current study is examining the clinical utility of manipulating the interphase gap (IPG) to estimate cochlear health (Prado-Guitierrez et al., 2006; Ramekers et al., 2014). These measures could theoretically be applied in human subjects to estimate neural health and predict speech recognition outcomes thereby overcoming issues related to a post-mortem approach. Further, ECAP data could be used to guide systematic manipulation of processor maps by activating or deactivating electrodes in order to maximize performance, an approach previously termed “site selection” (Garadat et al., 2013). However, before a site-selection approach using ECAP measures can come to fruition, further work is needed to determine the characteristics of the ECAP measures in human subjects and determine if it is feasible to use these measures on all electrodes among those who use a multichannel array.

The ECAP response represents the synchronous ensemble activity from electrically stimulated auditory nerve fibers, and is similar to Wave I of the electrically evoked auditory brainstem response (EABR). It consists of a negative (N1) and a positive (P2) peak, which occur approximately 0.2–0.4 ms and 0.6–0.8 ms following stimulus onset, respectively (Brown et al., 1998; Abbas et al., 1999). Several characteristics of the ECAP could potentially be examined to glean information regarding cochlear health; these measures include N1 latency, the amplitude of the response (voltage difference of N1-P2 peaks), and the slope of the amplitude-growth function (AGF; output amplitude vs input amplitude). It is hypothesized that the latency of the ECAP peaks, primarily N1, at high intensity levels convey information about the site of excitation along the neuron. At high stimulation levels near saturation, the N1 latency is shorter in cases of poorer neural health, as the site of excitation along the neuron moves to the to the central axon (Stypulkowski and van den Honert, 1984). Of note, a coexisting cause of decreased latency as a function of increasing stimulus level occurs simply due to faster excitation which is independent of neural health of site of excitation. The amplitude of the ECAP response or Wave I of the EABR (typically measured at a high stimulation level), has been shown to largely reflect the function, or health, of the stimulated neurons (Hall, 1990; Shepherd and Javel, 1997). Similarly, others have reported that the slope of the ECAP or Wave 1 ABR AGF is also correlated with SGN density (Smith and Simmons, 1983; Hall, 1990; Pfingst et al., 2014, 2015; Ramekers et al., 2014).

Of interest to the current study is the effect of IPG duration on the ECAP response across a multichannel electrode array. Increasing the IPG results in a reduction in the thresholds of auditory nerve fibers (Shepherd and Javel, 1999), lowers psychophysical detection thresholds in human CI recipients (Carlyon et al., 2005) and can cause increases in loudness perception, when all other stimulus parameters are held constant (McKay and Henshall, 2003). Further, the effects of IPG on the ECAP response are thought to be dependent on membrane characteristics, and thus reflect temporal response properties of the auditory nerve (van den Honert and Mortimer, 1979). It has been proposed that the relative change in suprathreshold characteristics of the ECAP response (e.g., amplitude, AGF slope, and N1 latency) due to manipulation of the IPG could be a clinically-useful tool for multichannel CI recipients as it theoretically could reflect within-channel attributes of neural health (Ramekers et al., 2014).

One limitation of using ECAP measures to assess neural health is that the recorded potentials will be influenced by conditions between the neurons and the recording electrode. The distance between the neurons and the electrodes as well as characteristics of the tissue between the neurons and the electrodes (fibrous tissue and or new bone) can vary along the electrode array and affect the ECAP recording. Therefore, particular characteristics of the ECAP that have been shown to relate to SGN density (e.g., peak amplitude and AGF slope) might reflect other variables in addition to neural health. It is not possible to characterize all of the conditions affecting the current paths between the neurons and the recording electrodes, particularly in living subjects. However, we can estimate some of these conditions by assessing the impedances for individual electrodes. High impedances, for example, might reflect the accumulation of denser tissue (fibrous tissue or new bone) near the recording electrode, resulting in lower ECAP responses. Examining how these ECAP characteristics change as the IPG increases may provide a method of estimating neural health which is less affected by conditions between the neurons and the electrodes. ECAP growth functions (slope or maximum amplitude) for short and long duration IPGs would presumably be affected in similar ways by the conditions near the recording electrode and these effects would cancel out when calculating the difference between two growth functions at a given recording site.

Prado-Guitierrez and colleagues measured ECAP AGFs in 15 deafened and implanted anesthetized animals (Prado-Guitierrez et al., 2006). The authors reported that the current level required to evoke an ECAP response with equal amplitude was always lower for pulse with a longer IPG (58 μs compared to 8 μs), but this effect was smaller in animals with poorer SGN density. In a related study, Ramekers and colleagues (Ramekers et al., 2014) measured the effects of varying the IPG on ECAP AGFs in eighteen anesthetized guinea pigs with CIs. Results showed increased excitability with increases in IPG across all animals, as measured by changes in several measured ECAP attributes. For example, results from Ramekers and colleagues showed that larger increases in the ECAP peak amplitude response as a function of increasing the IPG were negatively correlated with SGN density and perikaryal area. While the AGF slope data reported by Ramekers et al. (2014) appear to have the opposite pattern as the peak amplitude data reported above, this might be simply due to a difference in calculation: the effect of the IPG on the peak amplitude responses were calculated as a proportion of the peak amplitude with the shorter IPG, whereas the effects of the IPG on the AGF slope were calculated using raw values. One might also expect a similar negative correlation for the AGF slope analysis as was observed in the peak amplitude analysis if calculated as a proportion. Increasing the IPG generally caused increases in N1 latency values, particularly for the completely deafened animals with poorer SGN density. Animals with lower SGN density and perikaryal area were also shown to

have a greater expansion of the ECAP dynamic range as the IPG increased, when compared to animals with better neural health. Lastly, increasing the IPG resulted in a lower current level which corresponded with the 50% point along the AGF psychometric curve for nearly all animals, but this shift tended to be greater in animals with better neural health. It should be noted that the change in ECAP threshold as the IPG was increased was not strongly related to neural health characteristics. This last finding is in keeping with a recent report by DeVries and colleagues (DeVries et al., 2016) who reported that ECAP thresholds, but not amplitudes, measured in human subjects were significantly correlated with electrode position within the cochlea (e.g., distance between the electrodes and the modiolus). Taken together, these findings suggest electrode position may significantly contribute to threshold (or near threshold) measures, but measures obtained at higher current stimulation levels reflect, at least in part, neural health.

To date, the effects of IPG on ECAP measures have not been systematically investigated in human cochlear implant recipients, although based on animal studies this measure shows promise for clinical application in human subjects. However, it is first important to understand how manipulation of the IPG affects ECAP responses across a multichannel electrode array and if it is feasible to record responses on the majority of electrodes. In deafened human subjects, it is known that both the health of the neural population and the distances from the electrodes to the neurons vary along the length of the cochlea in a subject-specific manner (Nadol, 1997; Long et al., 2014; DeVries et al., 2016). Thus we hypothesized that suprathreshold ECAP measures that reflect cochlear health and or characteristics of the electrode-to-neuron current path would vary along the CI electrode array in a subject specific pattern. In the present study, we examined the effects of IPG on ECAP peak amplitudes and AGF slopes. The sampling rate used in the present study did not allow for sufficiently precise interpretation of N1 latency values. Second, since both measures studied here have been significantly related to SGN density (Ramekers et al., 2014) we expected that the measures would be somewhat, although not perfectly, correlated with one another across electrode sites. However, the effect of the IPG on each ECAP measure also inherently reflects the temporal response properties of the auditory neurons. Third, we examined how the across-site variance in simple impedance measures related to suprathreshold ECAP measures. We hypothesized that impedance values would correlate to some extent with across-site ECAP measures for a constant IPG; but, that perhaps a weaker or less frequent relationship would be observed between impedance values and across-site changes in ECAP measures as the IPG is increased. Lastly, we hypothesized that if suprathreshold characteristics of ECAPs do reflect neural density and it is has been shown that neural density degrades as a function of duration of hearing loss in humans (Nadol, 1997), then we should also find a significant relationship between ECAP measures and duration of hearing loss.

2. Subjects and methods

2.1. Subjects

Subjects were 10 bilaterally cochlear implanted users with peri- or post-lingual sensorineural hearing loss. The ears were implanted with Nucleus CI24R(CA), CI512 or CI24RE(CA) devices, all of which used a contour-advance precurved electrode array. Demographic information for the subjects is shown in Table 1. Note that four subjects were implanted at other institutions, and therefore detailed surgical history is not available. For those implanted at the University of Michigan Cochlear Implant Program, we have documentation that all electrodes were fully inserted. For those four that were implanted at other clinics, all electrodes were fully inserted per subject report. Additionally, there were no electrodes that met the definition for shorted or open circuits.

Lastly, it should be noted that 2/20 ears tested underwent explanation and reimplantation of their CI device (denoted using an asterisk in Table 1). In the case of s104 (L), the first device (CI24RECA) was implanted in 2009. She performed unexpectedly poor with the device. Therefore, this device was explanted and a new device (CI512) was implanted in 2010. Manufacturer analysis of the device was normal and integrity testing was normal. She performs similarly with the reimplanted device compared to the original device. In the case of s106 (L), the first device (CI24RCA) was implanted in 2000. The device was diagnosed as a hard failure in 2005, and therefore she was reimplanted (CI24RECA) at that time. It should also be noted that both ears were post-meningitic.

Table 1
Demographic data for each subject. The asterisks indicate history of explanation and reimplantation of the electrode array. The years of implantation in those cases reflect the duration of time since the first implant received.

	Age	Ear	Implant	Age at onset of hearing loss	Years of implantation	Etiology	Surgical approach
s81	64	R	CI24RE(CA)	39 years old	10	Hereditary	Not available
		L	CI24RE(CA)	39 years old	8		Not available
s89	70	R	CI24R(CA)	8 years old	11	Hereditary	Cochleostomy
		L	CI24RE(CA)	8 years old	6		Cochleostomy
s99	48	R	CI24RE(CA)	5 years old	3	Measles	Modified round window cochleostomy
		L	CI24RE(CA)	5 years old	2		Modified round window cochleostomy
s100	75	R	CI512	5 years old	5	Unknown	Not available
		L	CI24RE(CA)	5 years old	3		Not available
s101	63	R	CI512	35 years old	5	Auto-immune	Not available
		L	CI24RE(CA)	35 years old	9		Not available
s103	73	R	CI24RE(CA)	40 years old	0.5	Hereditary	Cochleostomy
		L	CI24RE(CA)	40 years old	1		Cochleostomy
s104	48	R	CI24R(CA)	3 years old	11	Hereditary	Cochleostomy
		L	CI512	3 years old	6*		Cochleostomy
s106	23	R	CI24RE(CA)	4 years old	3	Meningitis	Cochleostomy
		L	CI24RE(CA)	4 years old	13*		Cochleostomy
s107	64	R	CI24RE(CA)	5 years old	9	Hereditary	Cochleostomy
		L	CI512	5 years old	5		Cochleostomy
s108	25	R	CI24R(CA)	Congenital	1	Connexin 26	Not available
		L	CI24RE(CA)	Congenital	11		Not available

The left ear (first implanted) had minimal ossification at the time of implantation. The right ear (second implanted) was reported to have extensive ossification in the basal and apical turns which required extensive drilling away of the bone during surgery. A full insertion was achieved.

All subjects were native speakers of American English. The use of human subjects in the study was reviewed and approved by the University of Michigan Medical School Institutional Review Board.

2.2. Electrically evoked compound action potentials (ECAPs)

ECAPs were measured on each available electrode, within each ear, for all subjects. ECAPs were not measured on electrodes which were deactivated in the subjects' everyday clinical MAP. Of the electrodes for which ECAPs were measured, the AGF could not be assessed on 11% of the total number of electrodes and conditions (7 or 30 μs IPG) tested across subjects due to compliance limitations, restricted dynamic range, or poor morphology of the waveform. Most commonly, these electrodes consisted of the two or three most basal electrodes within the array for each ear (electrodes 1–3).

2.2.1. Method

ECAPs were measured with CustomSound EP Versions 4.2 and 4.3 software using Neural Response Telemetry. A laboratory owned CP910 speech processor connected to a desktop computer through a commercially available programming pod was used for data collection. Prior to measuring AGFs, the maximum stimulation level was determined on each electrode for each subject using the 'stimulate only' feature in the software. The measured maximum stimulation level for each electrode was used as the upper limit of stimulation when measuring the AGFs. Here, the maximum stimulation level was the highest current level that the subject reported as comfortable. Typically, subjects reported the maximum stimulation level as very loud but tolerable. Because manipulation of the IPG can affect loudness, the maximum stimulation level was measured for both 7 and 30 μs IPG conditions.

The 'amplitude-growth function' measurement available within the software was used to obtain each AGF. The dynamic range of stimulation for the AGFs differed in absolute current level for each electrode. The lower end of the dynamic range of stimulation was always a current level below the level required to elicit an ECAP response. The upper end of the dynamic range of stimulation was equal to the maximum stimulation level, as defined in the previous paragraph. The current level step sizes varied from 3 to 5 clinical units (CUs) depending on dynamic range (smaller step sizes used for a smaller dynamic range) in order to obtain a sufficient number of data points for curve fitting. The step size calculated in μA depended on the specific current levels used. For CI24RE(CA) and CI512 devices, IμA = 17.5 μA × 100^(CU/255). For CI24R devices we used a generic conversion, which assumed CU_0 = 10 μA, CU_{255} = 1750 μA, and that the average calibration value for the maximum allowable stimulation current level = 1910 μA. Given those assumptions, IμA = 10 × (1910/1750) × 175^(CU/255). Three data points were required to fit the slope function. For each recording, the peak-to-peak ECAP amplitudes were measured from the leading negative peak (N1) to the following positive peak (P2) using the CustomSound EP software. The AGF for each electrode was measured 2–3 times for each condition (7 and 30 μs IPGs, as outlined below), and average peak-to-peak amplitudes were calculated for each electrode, for each condition. Only those ECAP recordings with amplitudes above the level of the noise floor were included for analysis (Noise floor = 20 μV for CI24R; 5 μV for CI24RE and CI512).

2.2.2. ECAP recording parameters

For most recording parameters, the default settings of the software were used: 80 Hz rate, MP1 (extracochlear monopolar ball electrode) served as the probe & masker indifferent electrode, and the MP2 (extracochlear monopolar plate electrode) served as the recording indifferent electrode. The sampling rate was 20 kHz (one sample every 50 μs). The recording indifferent electrode was almost always located two electrodes apical to the probe electrode (e.g., if probe = electrode 10, then recording = electrode 12) when the probe electrode varied between electrodes 1–20. When the probe electrode was 21, then the recording electrode was 22. When the probe electrode was 22, then the recording electrode was 21. However, slightly alternative configurations were used for cases in which this default recording electrode was a deactivated electrode not used in the current study. For example, for s81 (L) electrodes 19–20 were deactivated and therefore the recording electrode was 18 or 21 when the probe electrode was 17 or 18, respectively. In any case, the recording electrode was never located more than three electrodes from the probe electrode. The number of sweeps for one recording varied from 50 to 200. The leading phase of the biphasic pulse for both the probe and the masker was always cathodic. The default gain and delay for both CI512 and CI24RE(CA) electrodes are 50 dB and 122 μs, respectively. The default gain and delay for the CI24R(CA) electrode are 60 dB and 55 μs, respectively. For most electrodes, these default gain settings were used, however, in some cases these parameters were adapted in order to improve the visibility of the N1 peak or morphology of the signal. For most subjects, the default pulse phase duration of 25 μs was used. For two subjects (s106 and s100) the phase duration was increased to 37 μs in order to achieve levels adequate for recording the ECAP response. Regardless, the pulse phase duration remained constant within a subject, across ears and across all electrodes. As noted above, the IPG of the biphasic pulse was either 7 or 30 μs, depending on the condition. A forward-masking technique was used for artifact cancellation (Abbas et al., 1999, 2004). The probe and masker active electrodes were always co-located; the masker level was always 10 CUs higher than the probe level. The masker probe interval was 400 μs.

2.3. Impedance measures

Simple impedance measures were performed on each electrode for each subject using the 'measure impedance' function in Custom Sound EP. The stimulus parameters were consistent for every electrode: the pulse rate was 228 pps, current level was equal to 80 CUs (74 μA), the pulse width was 25 μs, and the interphase gap was 8 μs/phase. The voltage at the end of the first pulse was measured and the impedance calculated as R = V/I (where R = resistance measured in Ohms, V = voltage, and I = current). Note that these simple impedance measures to not differentiate the amounts of resistive and reactive (capacitive) components that contribute to the total impedance values.

2.4. Statistical analysis

All data were analyzed using Sigmaplot Version 10.0 and SPSS Version 22. Prior to analyses, the measures of current ('clinical units') used in the CustomSound EP system was converted to microamps (μA). The key variables of interest for each ECAP input-output function were the peak amplitude and AGF slope. The linear slope ($y = y0 + ax$) was derived by determining a best-fit line through all data points that increased as a function of current level, recorded above the noise floor of the system. Examples of ECAP recordings are shown in Fig. 1 for two ears. The left panel in Fig. 1 shows an ECAP AGF for one electrode [s103 (R), Electrode 6]

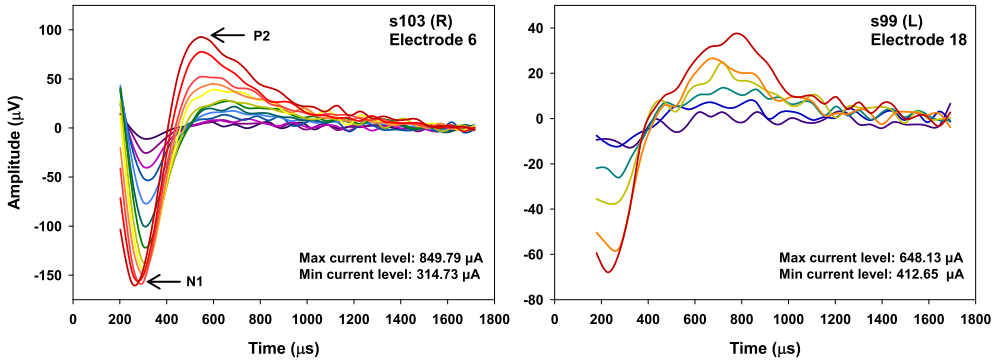

Fig. 1. Examples of typical acceptable waveforms recorded in the current study. The figure on the left shows an example of a robust response with a larger amplitude and dynamic range. The figure on the right shows an acceptable tracing, but with a lower overall amplitude and narrower dynamic range. Various colors corresponding with the color spectrum represent different input current levels; both the minimum (violet) and maximum (red) levels used to achieve these tracings are provided within each panel. (For interpretation of the references to colour in this figure legend, the reader is referred to the web version of this article.)

which demonstrated very robust, clean responses with a large dynamic range, while the right panel in Fig. 1 [s99 (L), Electrode 18] shows an ECAP AGF with acceptable morphology and a narrower dynamic range. Note that in both cases both an N1 and P2 response are present, with no indication of significant artifact. For the current study, all ECAP AGFs were required to show similar morphology with no indication of significant artifact.

For electrodes which showed a non-monotonic response at high levels, the linear slope was derived by including all data points above the noise floor, which increased in output value (μA) up to the level which produced a decrease in the N1-P2 amplitude relative to that produced by the next lower stimulus level. At least three points were required to fit the linear slope function. Examples of AGFs for two ears are shown in Fig. 2. It can be observed that a variety of curves are present across electrodes. In some cases, close to threshold, a shallower slope was observed before becoming steeper with increasing current level. Regardless, these points were included in the linear fit in order to maintain uniform criteria across all electrodes. However, only linear fits which were statistically significant and produced a regression coefficient (R^2) of 0.95 or higher were included in the analyses. We found that in every case, these criteria were met. It was found that most AGFs were monotonic and therefore could be fit with a linear slope equation, but not always a non-linear equation (e.g., sigmoidal fit). Therefore a linear equation was used for all electrodes. Fig. 3 provides an example of two AGFs obtained for one subject (s104) in the current study and shows how linear slopes were fit for cases in which the function was non-monotonic (e.g., electrode 21). The peak amplitude was defined as the maximum value of the N1-P2 amplitude for an AGF on each electrode. Typically, the peak amplitude occurred at the highest stimulation level. However, in cases of non-monotonicity (as previously discussed), the peak amplitude occurred at a stimulation level lower than the highest stimulation level.

The peak amplitudes and AGF slopes were calculated for each IPG at each electrode in both ears of all subjects. For some analyses, the average value was calculated across the entire electrode array to derive an across-site mean (ASM). Within each electrode, the changes in peak amplitude and AGF slope were calculated as the IPG was increased from 7 to 30 μs. The change (increase or decrease) in amplitude and slope as a function of the IPG was calculated as a proportion relative to the response for the 7 μs IPG. We used a proportional calculation to maintain consistency with (Ramekers et al., 2014) who used the same method to determine the effects of the IPG on ECAP amplitudes.

3. Results

3.1. Peak amplitude (N1-P2)

Fig. 4 shows the mean values for the peak amplitude (N1-P2 in μV) for each subject and for each available electrode. Each graph represents results from an individual subject. Note that the y-axis scale differs for each subject due to the large variation in amplitude across subjects. Within each graph, results from both the right ear (circles) and the left ear (triangles) and IPG conditions of 7 μs (dark red or blue) and 30 μs (lighter red or blue) are shown.

It is apparent from Fig. 4 that the N1-P2 peak amplitudes varied across stimulation sites and also across ears within a subject. A two-

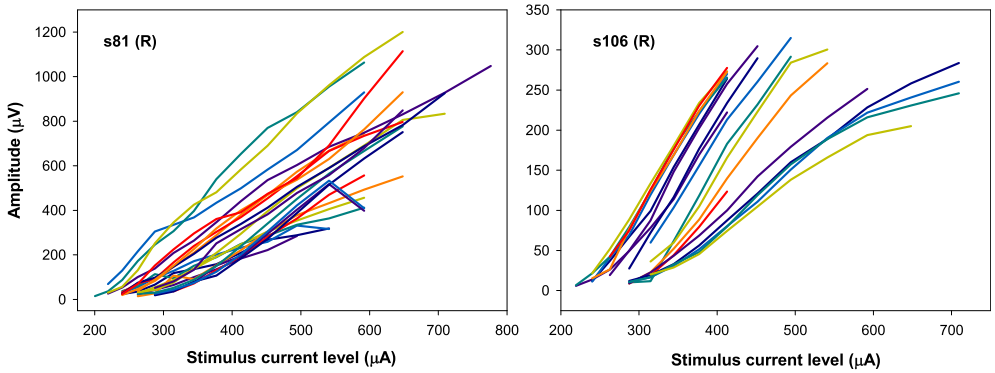

Fig. 2. Examples of ECAP AGF functions for two ears evaluated in the current study. In both examples shown, the IPG was equal to 7 μs. Within each panel, the colors represent results obtained on different electrode locations within the electrode array, but not in a systematic manner (e.g., colors were chosen at random and do not correspond to a specific electrode number, place or order).

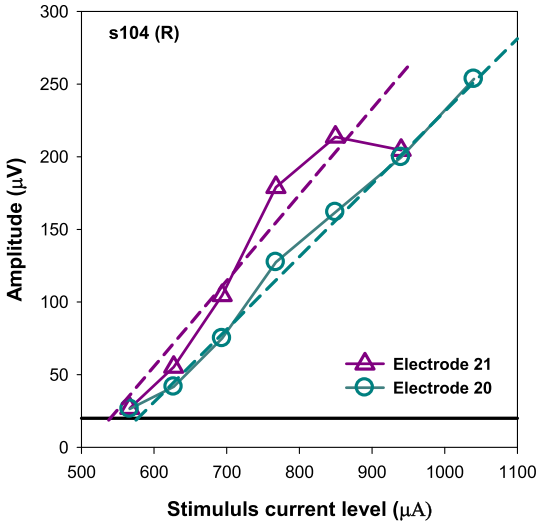

Fig. 3. Examples amplitude-growth functions (AGFs) are shown for one subject (s104). Results are shown for adjacent electrodes in the right ear. The AGF for electrode 20 (open green circles) was the most common pattern observed across all electrodes tested in the current study. The green dashed line shows the linear slope function for this AGF. The AGF for electrode 21 (open purple triangles) was less commonly observed across all electrodes tested. In this case, the linear slope function was fit from all points above the noise floor to the maximum N1-P2 value in the AGF; in this case, the maximum N1-P2 value did not occur at the highest stimulation level. The purple dashed line shows the linear slope function for this AGF, which was based only on data points up to the maximum N1-P2 value. (For interpretation of the references to colour in this figure legend, the reader is referred to the web version of this article.)

way ANOVA was performed within each ear to determine how electrode number (site of stimulation) and IPG condition affect ECAP peak amplitudes. For all subjects, results showed a significant main effect of electrode number showing that the peak amplitude values varied significantly across electrodes for each listener when collapsed across ears and IPG duration ($p < 0.05$). Additionally, one-way ANOVA revealed a significant main effect of electrode within each ear for each IPG condition ($p < 0.01$) for all subjects. A significant interaction (electrode number × IPG duration) was also noted for each subject suggesting that the effects of the IPG on the peak amplitudes are dependent on the electrode ($p < 0.01$). In all cases there was no generally consistent effect of electrode location on the IPG effect; patterns were complex and varied across ears.

Fig. 5 shows the across-site patterns of the proportional change in peak amplitude as the IPG was increased from 7 to 30 μs for both ears within each subject. Note that the y-axis scale differs for each subject due to the large variation in amplitude across subjects. A dashed horizontal line is provided as a reference and is equal to zero. Data points falling along this line would suggest no effect of IPG on the ECAP peak amplitude. A one-way ANOVA performed within each ear tested revealed a significant main effect of electrode site location on the proportional change in peak amplitude for each ear tested ($p < 0.05$). It should also be noted that for some electrodes, increasing the IPG decreased the peak amplitude. It can be observed that in some ears [e.g., s99 (L)] a significant number of data points are missing. Recall that the within-electrode change in peak amplitude as the IPG was increased from 7 to 30 μs was calculated using current stimulation levels that were equal for both IPG conditions (e.g., the highest possible stimulation level that was equivalent in both 7 and 30 IPG conditions within an electrode). Therefore, in some cases, such as s99, current stimulation levels did not overlap within an electrode, across IPG conditions and therefore the change in peak amplitude could not be calculated.

We examined the ASM differences for each ear as a function of the IPG duration for the highest possible stimulation level that was equivalent in both 7 and 30 IPG conditions within an electrode. The average N1-P2 peak amplitude across all subjects (all electrodes and IPG conditions for 16 ears) was 220.72 μV (SD = 210.09). Note that the four ears that were tested using a 37 μs/phase biphasic pulse were not included to calculate these descriptive statistics. The top graph in Fig. 6 shows the ASM peak amplitude values for each subject for each condition when current levels were equal across IPG conditions within an ear; the bottom graph in Fig. 6 shows the proportional change in voltage of the N1-P2 response as a function of the IPG duration when equalized for current stimulus level. The ASM peak amplitudes also varied across subjects, with the highest average amplitude levels of more than 900 μV (s81) while some of the lowest average peak values were less than 30 μV (s89 and s99). Despite the fact that within some electrodes increasing the IPG resulted in a decrease in peak amplitude (Fig. 5), there was generally a positive change in peak amplitude with increased IPG duration when averaged across all electrode sites within an ear (bottom graph, Fig. 6). To confirm this observation, a one-sample, 2-tailed *t*-test was calculated for each ear and it was found that a change in proportional amplitude was significantly different from zero ($p < 0.05$) in all cases except for s106 (both ears) and s100 (left ear only).

3.2. Linear slope

Fig. 7 shows the raw mean values for the linear slope fits for the AGFs for each subject for each available electrode. Symbols are consistent with those reported previously for Fig. 4. The magnitudes of linear slope values varied considerably across subjects ranging from <0.2 μV/μA to >3 μV/μA. The average slope value across all subjects (for 16 ears and electrodes and IPGs) was 0.66 μV/μA (SD = 0.51). Note that four ears that were tested using a 37 μs/phase biphasic pulse were not included to calculate these descriptive statistics.

Similar to previous findings reported in Fig. 4, results in Fig. 7 show that the across-site patterns of linear slope functions also differ significantly across subjects and across electrodes. A two-way ANOVA was performed within each subject to determine how electrode number (site of stimulation) and IPG condition affect ECAP AGF slopes and revealed a significant main effect of electrode for each subject supporting the observation that linear slope functions of the AGF differ significantly across electrodes ($p < 0.01$). The across-site patterns of the effect of increasing the IPG on the linear slope for each ear are shown in Fig. 8. Similar to Fig. 5, note that the y-axis scale differs for each subject due to the large variation in amplitude across subjects. Also in keeping with Fig. 5 (peak amplitude data), for some electrodes, increasing the IPG decreased the AGF slope. Based on observation, it appears that the effect of the IPG on AGF slope differs depending on electrode site location, but response patterns vary across ears tested. This observation was confirmed as a one-way ANOVA performed within each ear tested revealed a significant main effect of electrode site location on the proportional change in AGF slope for each ear tested ($p < 0.05$).

The ASM effect of increasing the IPG on the linear slope is shown in Fig. 9, in which the top graph shows the ASM linear slope values for each subject for each condition; the bottom graph in Fig. 9 shows the proportional change in the linear slope as a function of the IPG duration. Similar to the peak amplitude data reported above (Fig. 6, bottom graph), there was generally a positive change in ASM slope with increased IPG duration when averaged across all electrode sites within an ear (bottom panel, Fig. 9). A one-sample, 2-tailed *t*-test calculated for each ear confirmed this observation: the change in slope was positive and significantly different from zero ($p < 0.05$) in all cases except for s100 and s104 in the left ear and for s106 in the right ear.

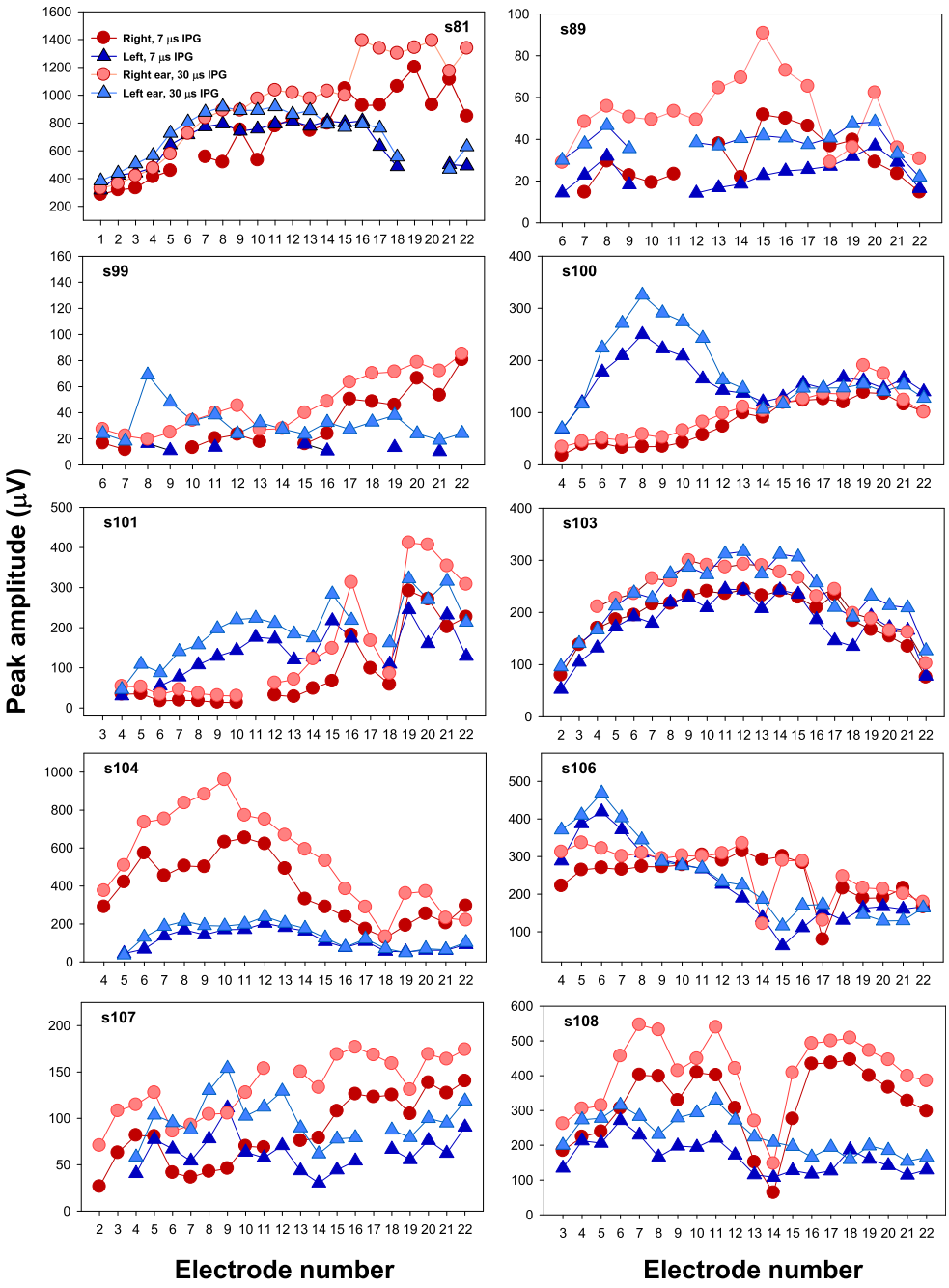

Fig. 4. Peak amplitude values in microvolts (μV), for each electrode for each ear. Each graph represents data obtained for both ears of a subject. Circles represent data obtained in the right ear and triangles represent data obtained in the left ear. The dark colors represent data for 7 μs IPG and the lighter colors represent data for 30 μs IPG. Missing data points represent cases in which ECAPs could not be accurately recorded, or, cases in which they were not recorded due to the fact that those electrode sites were deactivated in the subject's clinical speech processor MAP.

3.3. Comparison of ECAP measures across electrodes

In order to examine similarities in the across-site patterns of ECAP measures within each subject, correlation matrices (2-tailed, Pearson's product moment correlation coefficients) were calculated within each ear, for each subject. Data analysis was confined to within each ear in order to limit the number of multiple comparisons and because it is hypothesized that these measures are ear specific; the second point can be observed in Figs. 4 and 7 which demonstrate non-uniform across-site patterns of ECAP measures across both ears. Each matrix examined four variables [2 ECAP measures × 2 IPG durations (7 and 30 μs)] for six comparisons total. Therefore, a significant correlation was signified by a p-value <0.008. The change in each ECAP measure as a function of IPG was not included in the analysis since it was calculated as a proportional measure relative to the 7 μs IPG condition.

The correlational analyses were then examined across all subjects in both ears to identify common patterns of significance. It was observed that the most frequent significant correlations existed between IPG durations (7 and 30 μs) for a given ECAP measure: a) In 16/20 ears, the ECAP peak amplitude for a 7 μs IPG duration was significantly correlated with the ECAP peak amplitude for a 30 IPG

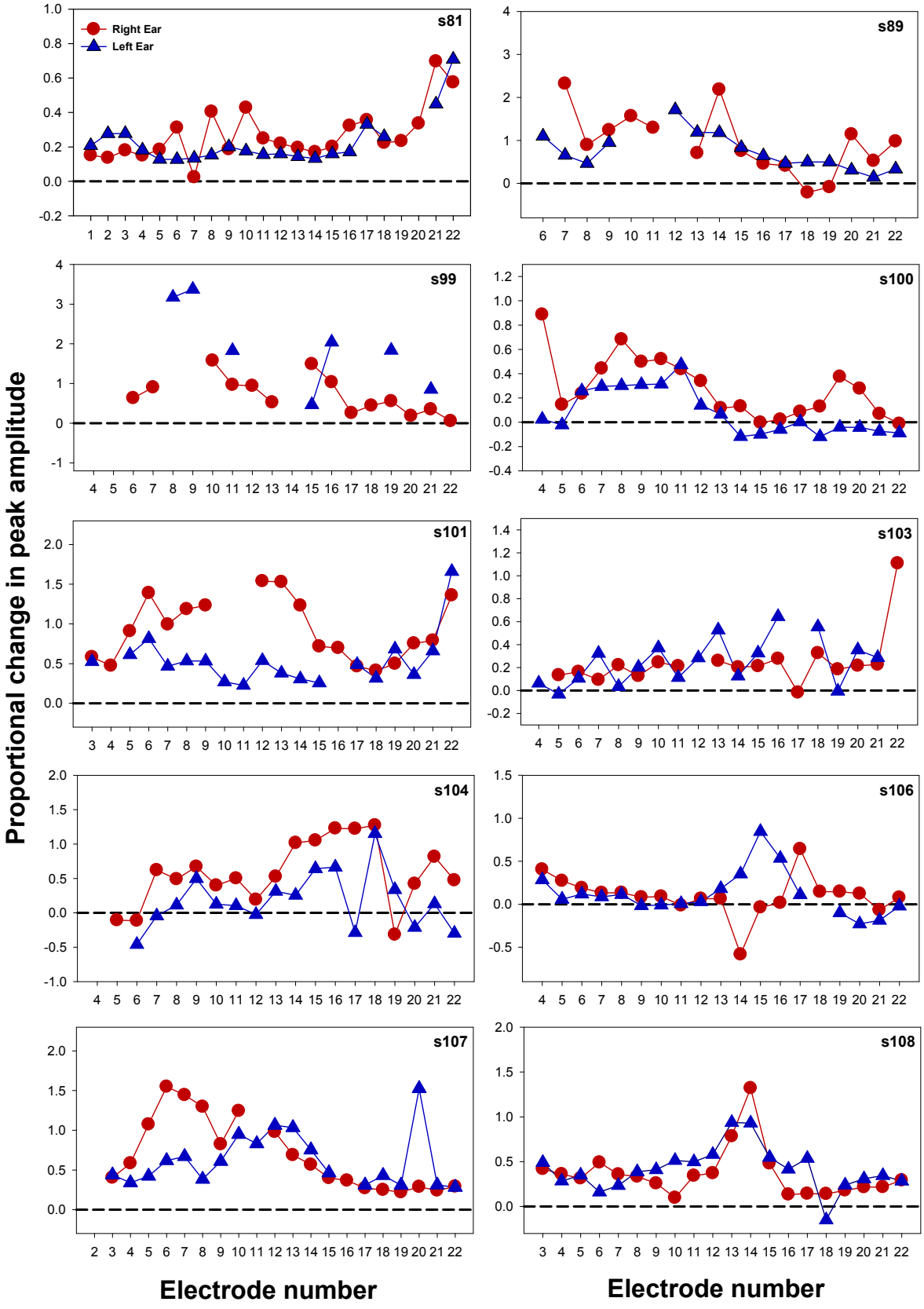

Fig. 5. Proportional change in peak amplitude as the IPG was increased from 7 to 30 μs, for each electrode in each ear tested. Red circles represent results obtained in the right ear and blue triangles represent results obtained in the left ear. Missing data points represent cases in which (1) ECAPs could not be accurately recorded; (2) cases in which they were not recorded due to the fact that those electrode sites were deactivated in the subject's clinical speech processor MAP; or (3) cases in which equal current stimulation levels did not occur across the 7 and 30 μs conditions. The dashed horizontal line is equal to zero, and is provided as a reference to better visualize the change in amplitude as the IPG was increased. (For interpretation of the references to colour in this figure legend, the reader is referred to the web version of this article.)

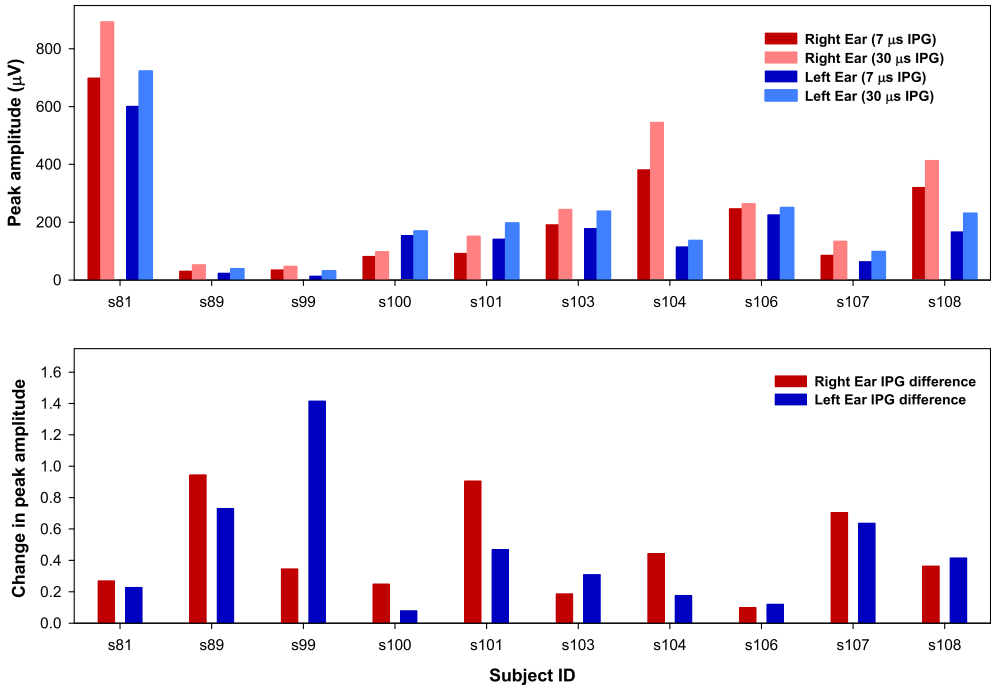

Fig. 6. The top portion of the graph shows the ASMs of the peak amplitude values for each IPG condition and ear for each subject. The bottom portion of the graph shows the ASM values for the change in the peak amplitude as the IPG increases from 7 to 30 μs for equal current levels. The change in the peak amplitude is calculated as a proportion of the peak amplitude at the 7 μs IPG condition for each electrode.

duration and b) in 16/20 ears, the ECAP linear slope value for a 7 μs IPG duration was significantly correlated with the ECAP linear slope value for a 30 IPG duration. Note, that for both of the above analysis, the 16 ears that showed a significant correlation for the peak amplitude data were not necessarily the same ears that showed a significant correlation for the AGF slope data. In both cases, correlation coefficients (r) ranged from 0.53 to 0.98. Additionally, the peak amplitude values and slope values tended to be significantly correlated regardless of IPG duration; in all four comparisons, the correlation was significant in 11–14 of the 20 ears depending on IPG condition. Taken together, these findings suggest that a) the 7 and 30 IPG conditions for each measure tend to be correlated with one another within each ear particularly for the peak amplitude and slope values and 2) the peak amplitude and slope values tended to be correlated with one another.

3.4. Impedance measures

Across-site variances in common ground, simple impedances are shown in Fig. 10. The red circles and blue triangles represent impedance values at every electrode site in the right and left ears, respectively. In order to determine the extent to which the across-site variance in impedance measures affects ECAP measures, correlation matrices (2-tailed, Pearson's product moment correlation coefficients) were completed between the across-site impedance measures of the recording electrode site and (1) ECAP peak amplitude or AGF slope for the 7 μs IPG conditions; and (2) how these characteristics change as the IPG was increased from 7 to 30 μs. In keeping with previous analysis, the peak amplitude and AGF slope changes as a function of the IPG increasing were calculated in proportions.

A correlation matrix for the first analysis is shown in Table 2 and the second (effect of IPG) is shown in Table 3. Note that corrected significance level for each analysis is $p < 0.0125$ given that each ear's impedance values were compared with four ECAP measures in a single ear (0.05/4); these results are merely divided into two tables for easier review and interpretation. A review of the results in Table 2 shows that there is a significant, negative relationship between ECAP measures using a 7 IPG μs IPG and impedance measures for 37.5% (15/40) of the analyses. These results suggest that in some cases higher impedance values are correlated with lower ECAP peak amplitude and/or linear slope values, or vice versa. The results comparing across-site impedances to how these measures change as the IPG is increased from 7 to 30 μs are shown in Table 3, and it can be observed that the results are quite different from those in Table 2. Specifically, a significant relationship was observed for only 2.5% (1/40) of the analyses. These results suggest, that, the influence of simple impedance values specific to an ECAP recording site is greater for ECAP measures using a constant IPG value (e.g., 7 μs) compared to examining how the ECAP measures changes as the IPG increases.

3.5. Duration of hearing loss prior to implantation

It is logical that if specific characteristics of the ECAP reflect neural health, then those features should also be related to the duration of hearing loss and/or deafness. For the current analyses it was decided to use the duration of hearing loss, as opposed to duration of deafness, given that more recently implanted CI recipients are not likely to be completely deaf prior to receiving a CI. Duration of hearing loss prior to implantation was determined based on patient self-report and was in years based on the age at which hearing loss was first identified. In all subjects, hearing loss was bilateral at the time of identification.

In order to examine the relationship between duration of hearing loss and characteristics of the ECAP measure, ASM values were calculated for each ECAP measure and IPG duration, within each ear. Since previous within-subject analyses showed that some of the specific features of the ECAP were highly correlated with one another, only a specific set of characteristics regarded to be

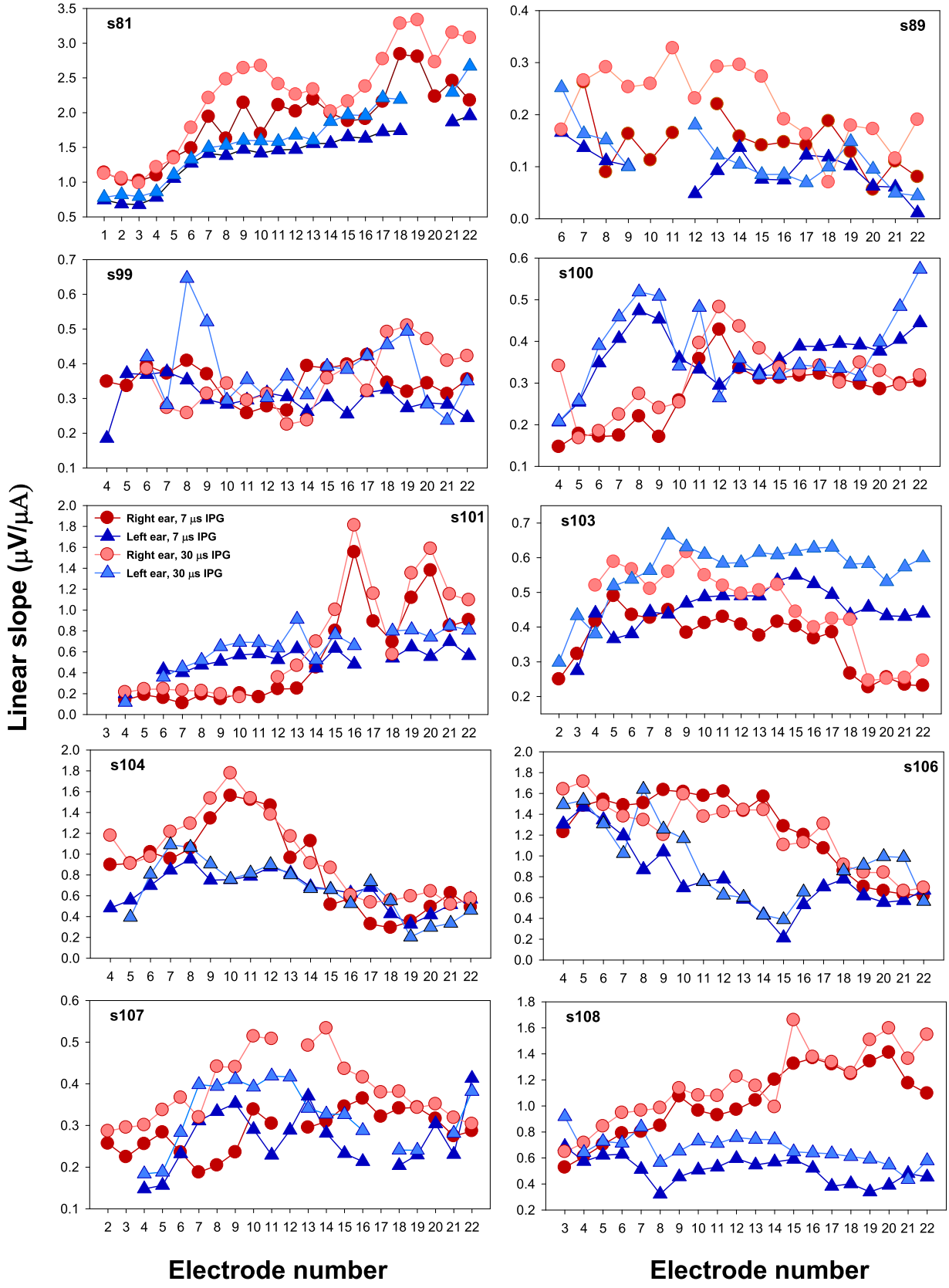

Fig. 7. Similar to Fig. 4, but representing the linear slopes for the AGFs for each electrode, in each ear, for each subject. Missing data points represent cases in which (1) ECAPs could not be accurately recorded; or (2) cases in which they were not recorded due to the fact that those electrode sites were deactivated in the subject's clinical speech processor MAP.

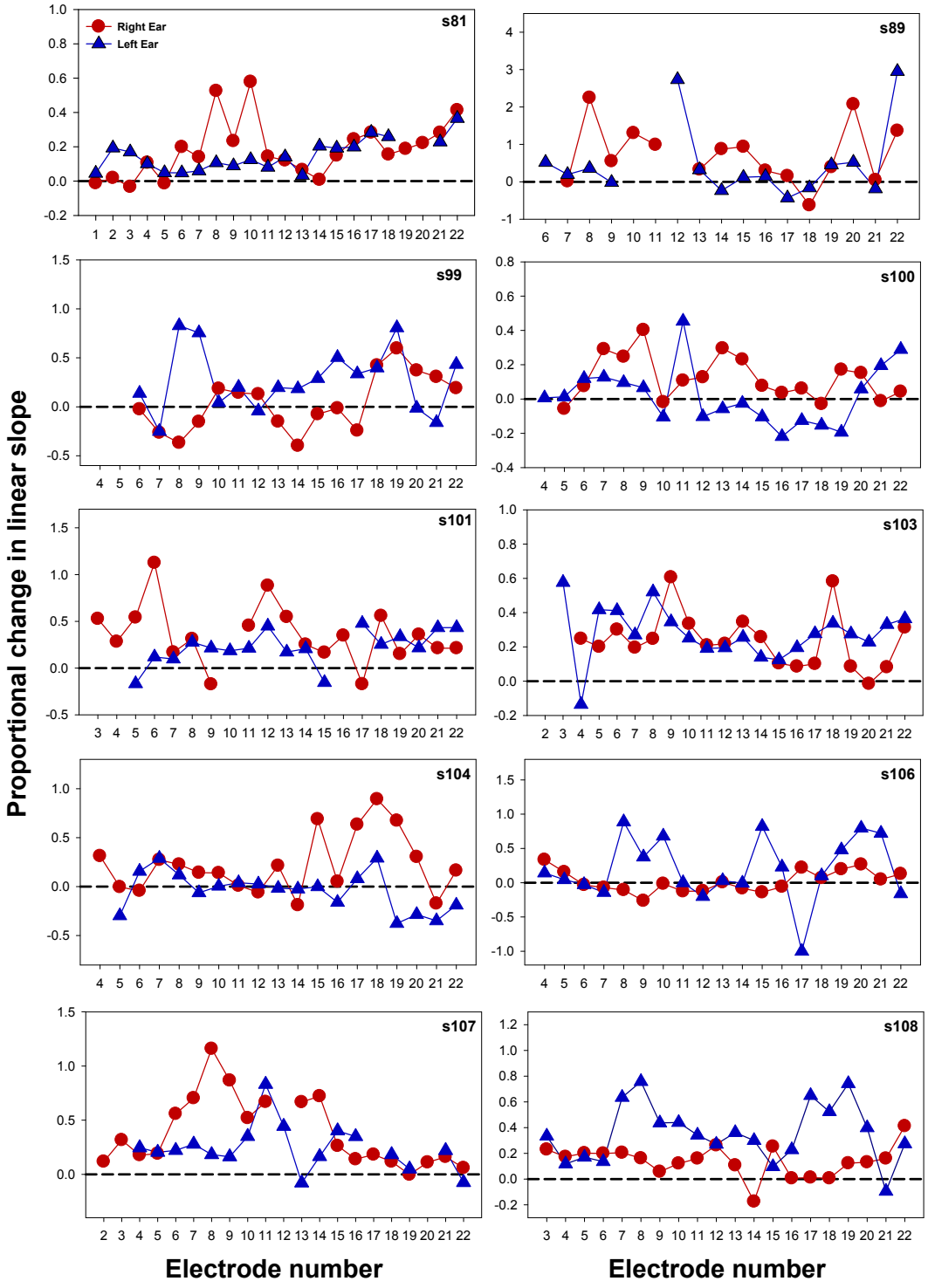

Fig. 8. Similar to Fig. 5 but data shown represents the proportional change in AGF linear slope as the IPG was increased from 7 to 30 μs, for each electrode in each ear tested.

relatively independent of one another were selected for analysis. Specifically, using 2-tailed, Pearson's product moment correlation coefficients we examined the relationship between duration of hearing loss and ASM values for (1) ECAP linear slope (7 μs IPG) and (2) magnitude of change in the ECAP linear slope as a function of increasing the IPG duration from 7 to 30 μs across all subjects (N = 20 ears). Therefore, a significance level (p value) was <0.025. Results are shown in Table 4. There was a significant negative correlation between the linear slope for a 7 μs IPG stimulus and the duration of hearing loss (years). This relationship is shown in Fig. 11. Red circles and blue triangles represent data from ten right and ten left ears, respectively. These results show a significant, negative correlation between AGF linear slope (7 μs IPG) and duration of hearing loss. Slopes tended to be steeper for shorter durations of hearing loss and shallower for longer durations of hearing loss. The correlation between duration of hearing loss and magnitude of

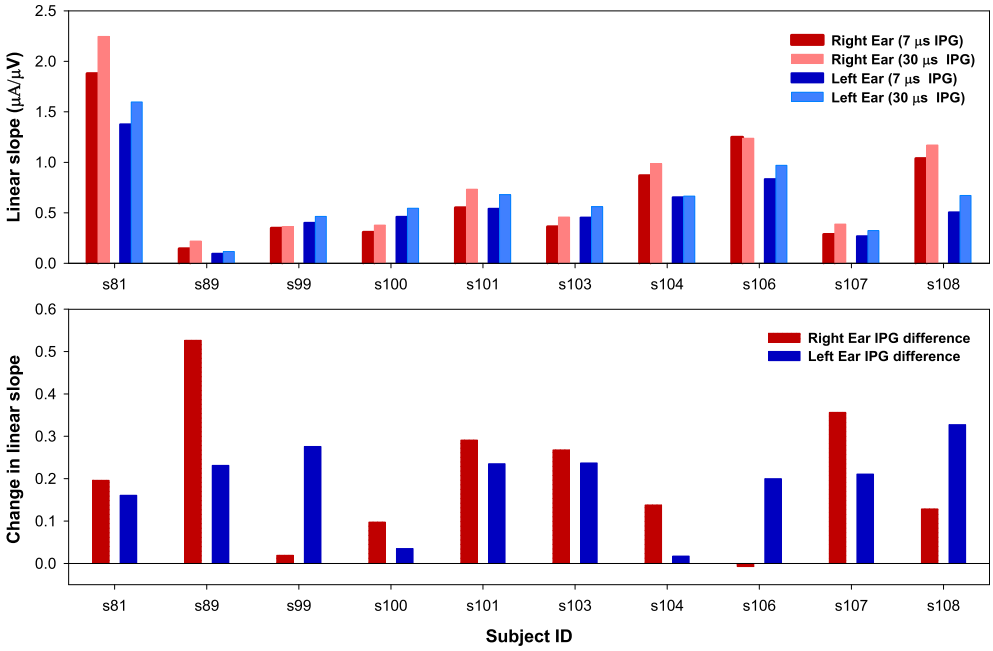

Fig. 9. Similar to Fig. 6, but representing the ASM linear slope values for the amplitude-growth functions on each electrode. In keeping with Fig. 6, the bottom portion of the graph reflects the change in linear slope as a proportion of the linear slope at the 7 μs IPG condition for each electrode.

change in the ECAP linear slope as a function of increasing the IPG duration was not significant, as noted in Table 4.

4. Discussion

4.1. Across-site patterns

In the current study, we examined two features of the ECAP in cochlear implanted adults, and how those features vary across electrodes and with varying IPG duration. In 89% of the electrodes, the ECAP AGF could be reliably measured. Similarly, Nehme and colleagues (Nehme et al., 2014) measured ECAP AGFs in 34 children and adults using the Advanced Bionics HiRes90K™ device and reported that these measures could be reliability obtained on 91% of the electrodes tested. Data were initially analyzed using several methods to include sigmoidal functions and an area under the curve analysis. However, the area under the curve estimate posed problems primarily due to non-uniform input dynamic range across electrodes and across subjects. Additionally, it was observed that a sigmoidal function, which is often found in studies in anesthetized animals, was fairly uncommon across all ears tested likely due to the fact that stimulation levels were limited by patient subjective comfort ratings. A linear slope function was found to be the most appropriate fit in the majority of cases across all electrodes and ears tested. For the rare cases in which the AGF was nonmonotonic, only the portion of the function up to the peak amplitude of the response was analyzed.

In general, it was observed that both features of the ECAP (peak amplitude or AGF slope) varied significantly across the electrode array in all ears suggesting that the measures are affected by localized biological or biophysical variables near each electrode. The amplitude change or slope of the ECAP AGF is thought to represent the number of neurons that respond to each incremental increase in current stimulation level. Significant across-site differences were also observed when examining the proportional change in peak amplitude or linear slope as the IPG was increased from 7 to 30 μs and therefore one could conclude that this measure also depends on localized variables near each electrode. Previous reports document that ECAP AGFs are generally steeper and amplitudes greater in the apical as opposed to the basal electrodes (Polak et al., 2004; Brill et al., 2009), but this was not found in all subjects in the current study. As noted in Figs. 4 and 7, the across-site patterns for both ECAP peak amplitude and AGF linear slope were diverse and varied both across-subjects and across ears. ECAP recordings reported in the current study seem to be fairly independent of internal device. For example, both s81 and s106 were implanted with CI24RE (CA) implants in both ears and showed markedly different across-site patterns. Subject s81 showed a pattern commonly reported in previous studies in which the peak-amplitude and slope values are higher in the apical electrodes and lower in the basal electrodes. However, a nearly opposite pattern was observed for s106. In fact, all ears tested ($N = 20$) were implanted with devices that had identical electrode arrays (Contour Advance) and showed highly individualized patterns. The variation in these patterns across subjects suggests that the patterns are, at least in part, dependent on the pattern of pathology or biophysical variables along an individual's electrode array rather than to normal differences in the apical-to-basal morphology that would be common to all subjects. It was also noted that in most ears the across-site variation in the peak amplitude of the ECAP was correlated with the across-site slope of the AGF. This finding is not necessarily surprising since a linear function was used to derive the slope for each electrode. Additionally, it was often observed that a specific ECAP measure for a shorter duration IPG (7 μs) was highly correlated across stimulation sites with the same ECAP measure obtained with a longer duration IPG (30 μs) within an ear.

4.2. Relationship with impedance measures

Interestingly, we found that the relationship between across-site variances in simple impedance values and ECAP measures depended on the specific ECAP measure. For example, we showed that the peak amplitude and AGF slope of the ECAP recording was

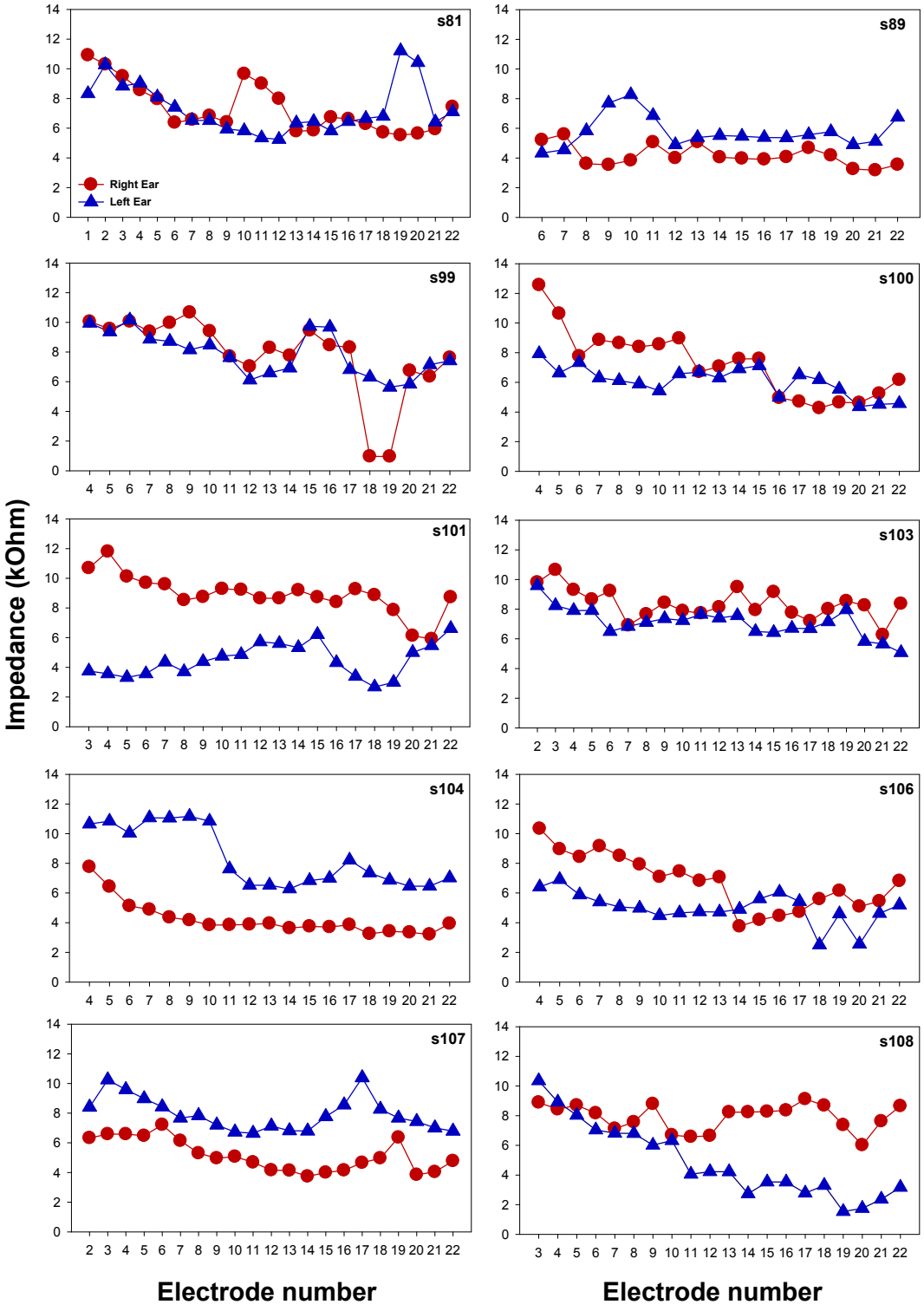

Fig. 10. Impedance values (kOhm) for each electrode for each ear. Each graph represents data obtained for both ears of a subject. Red circles represent data obtained in the right ear and blue triangles represent data obtained in the left ear. Note that here impedance values are shown for all electrodes, even those that were not used to measure ECAPs in the current study. Electrodes 18 and 19 in s99 (R) do indicate low impedance values but do not necessarily meet the threshold for abnormal electrode function (<0.5 kOhm), as defined by the manufacturer. (For interpretation of the references to colour in this figure legend, the reader is referred to the web version of this article.)

related to recording electrode impedance in 37.5% of the cases. However, the magnitude of change in the ECAP measure as a function of manipulating the IPG was only related to recording electrode impedance values in one comparison (see Tables 2 and 3). Therefore, this second ECAP measure which has been shown to be related to neural health in the cochlear implanted guinea pig may be a more ideal measure to implement clinically in human recipients with multi-channel arrays given that it is seemingly less affected by across-site variation in impedance values. The impedance measures obtained in the current study were measured using

Table 2
Matrix showing the results of the across-site correlational analyses between impedance values and ECAP peak-amplitude and AGF for a constant IPG of 7 μs. Results meeting criteria after Bonferroni corrected p values ($p < 0.0125$) are shown in bold with an asterisk(*).

	7 IPG peak amplitude		7 IPG AGF slope	
	R	L	R	L
s81	**r = −0.781**	**r = −0.756**	**r = −0.752**	**r = −0.773**
	p < 0.001*	**p < 0.001***	**p < 0.001***	**p < 0.001***
s89	r = −0.065	r = −0.278	**r = 0.869**	r = −0.303
	p = 0.818	p = 0.31	**p < 0.001***	p = 0.27
s99	**r = −0.677**	r = −0.125	r = 0.388	r = 0.103
	p = 0.003*	p = 0.610	p = 0.124	p = 0.675
s100	**r = −0.842**	r = −0.238	**r = −0.604**	**r = −0.575**
	p < 0.001*	p = 0.327	**p = 0.006***	**p = 0.010**
s101	**r = −0.697**	r = −0.281	**r = −0.607**	r = 0.379
	p < 0.001*	p = 0.275	**p < 0.001***	p = 0.134
s103	r = −0.306	r = −0.468	r = −0.029	r = 0.252
	p = 0.17	p = 0.032	p = 0.90	p = 0.28
s104	r = 0.402	r = −0.144	r = 0.196	r = 0.327
	p = 0.08	p = 0.17	p = 0.422	p = 0.17
s106	r = 0.023	r = 0.438	r = 0.381	r = 0.444
	p = 0.925	p = 0.060	p = 0.108	p = 0.057
s107	**r = −0.517**	r = −0.287	**r = −0.531**	**r = −0.696**
	p = 0.002*	p = 0.249	**p = 0.002***	**p < 0.001***
s108	r = −0.372	r = 0.036	r = −0.111	**r = −0.587**
	p = 0.106	p = 0.881	p = 0.642	**p = 0.012***

Table 3
Matrix showing the results of the correlational analyses between across-site impedance values and the change in ECAP peak-amplitude and AGF slope as the IPG was increased from 7 to 30 μs. Results meeting criteria after Bonferroni corrected p values ($p < 0.0125$) are shown in bold with an asterisk(*).

	IPG difference peak amplitude		IPG difference AGF slope	
	R	L	R	L
s81	r = −0.211	r = −0.208	r = −0.193	r = −0.314
	p = 0.022	p = 0.35	p = 0.39	p = 0.154
s89	r = 0.194	r = −0.418	r = −0.462	r = −0.037
	p = 0.022	p = 0.095	p = 0.083	p = 0.88
s99	r = 0.548	r = −0.008	r = −0.564	r = 0.028
	p = 0.065	p = 0.98	p = 0.049	p = 0.91
s100	**r = 0.629***	r = 0.203	r = 0.208	r = −0.098
	p = 0.004	p = 0.40	p = 0.40	p = 0.69
s101	r = 0.122	r = −0.073	r = 0.193	r = 0.347
	p = 0.63	p = 0.77	p = 0.44	p = 0.15
s103	r = 0.145	r = −0.339	r = 0.236	r = 0.002
	p = 0.58	p = 0.18	p = 0.33	p = 0.99
s104	r = −473	r = −0.170	r = −0.141	r = 0.346
	p = 0.047	p = 0.16	p = 0.56	p = 0.16
s106	r = 416	r = 0.514	r = 0.058	r = −0.262
	p = 0.077	p = 0.029	p = 0.81	p = 0.27
s107	r = −0.187	r = −0.244	r = 0.305	r = 0.050
	p = 0.43	p = 0.30	p = 0.19	p = 0.83
s108	r = 0.134	r = −0.085	r = −0.140	r = −0.088
	p = 0.57	p = 0.72	p = 0.556	p = 0.71

Table 4
Matrix showing the results of the correlational analysis between the duration of hearing loss for each ear tested (years) and (1) the across-site mean (ASM) of linear slopes of the amplitude-growth function for the 7 μs IPG condition or (2) the ASM change in linear slope of the amplitude-growth function (30-7 μs IPG). Results meeting criteria after Bonferroni correct p value ($p < 0.025$) are shown in bold with an asterisk(*).

	Linear slope (7 μs IPG)	Linear slope change (30-7 μs IPG)
Duration of hearing loss (years)	**r = −0.66***	r = 0.31
	p < 0.01	p = 0.17

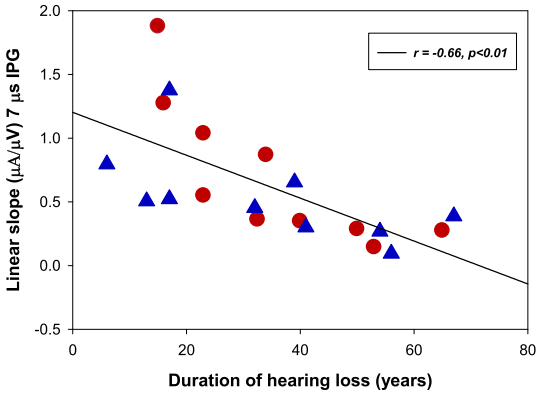

Fig. 11. Scatterplot showing the significant correlation between duration of hearing loss (years) and the ASMs for the linear slopes of the amplitude-growth functions for the 7 μs IPG condition, for each ear, for each subject. Each data point represents the across site mean for one ear (Right ear = red circles; Left ear = blue triangles). (For interpretation of the references to colour in this figure legend, the reader is referred to the web version of this article.)

clinically available software, which provides only a measure of simple impedance in kOhm. In fact, this cumulative impedance involves both resistance and reactive components, the latter of which may depend on the frequency of the signal and the geometry of the electrode surface (Tykocinski et al., 2001; Duan et al., 2004; Franks et al., 2005). The resistive component is thought to be largely determined by the properties surrounding the electrode (e.g, perilymph, fibrous tissue or bony growth) (Duan et al., 2004). Further work is needed to determine the extent to which specific impedance components influence ECAP recordings in human subjects.

It was noted that, while impedance measures were statistically significantly different across electrode sites within a multichannel array, it is possible that correlations not shown to reach statistical significance in Table 2 were due to the fact that the impedance measures varied less across electrode site compared to those correlations that did reach statistical significance. However, a cursory observation of the data does not necessarily support this reasoning. We examined the standard deviations of across-site measures in impedance for each ear and the correlations noted in Table 2 and did not observe any obvious trends. For example, results shown for s107 in Table 2 demonstrate that 3 out of the four correlation analyses showed significant results and the standard deviations of the across-site measures were approximately 1.09 and 1.13 for the right and left ears, respectively. However, similar impedance standard deviations were observed for s103 for whom no significant correlations were observed. Similar patterns were noted across the subjects, and overall did not suggest that variance in impedance affected the results reported in Table 2.

4.3. Effect of the inter-phase gap (IPG)

For each ECAP measure, the IPG was increased and the effect of this manipulation was measured at each electrode. For an equal current stimulation level, increasing the IPG duration resulted in significantly increased amplitude of the response at a given electrode when responses were averaged across the electrode array (Fig. 6). Likewise, increasing the IPG duration typically resulted in an increase in the linear slope of the AGF function for each electrode (Fig. 9). These observations are expected and consistent with the previous conclusions that increasing IPG duration increases excitability of the stimulated neuronal population (McKay and Henshall, 2003; Prado-Guitierrez et al., 2006; Ramekers et al., 2014). For the peak amplitude data (Fig. 6), the ASM proportional

change caused by increasing the IPG was noted to be more than double that of the peak amplitude for the 7 μs IPG response in some ears (e.g., s99), however it should be noted that this average was calculated from a relatively small sample size as shown in Fig. 5 (s99). This is further discussed below. In other cases, this proportional change was quite small (<0.2). As noted for s99 in Fig. 5, measuring the effect of IPG on ECAP amplitude for equal current levels may be problematic. As discussed previously, for this subject increasing the IPG to 30 μs caused such a marked decrease in the entire dynamic range for certain electrodes that none of the stimulus current level ranges for the AGF functions overlapped across the two IPG conditions. This strong effect was not observed for any other subject, however, this should be taken into consideration when considering which ECAP measures might be appropriate for clinical applications. For example, it can be noted that for the same subject the effect of the IPG on ECAP linear slopes could be calculated without issue on all electrodes (Fig. 8) which may argue in favor of using such a measure in future clinical applications.

In keeping with peak amplitude data (Fig. 5), results show that the effect of IPG on AGF slopes did vary across electrodes and in some cases increasing the IPG resulted in a decrease in amplitude or linear slope, as shown in Fig. 8. Regardless, these results show that the ASM values typically increase for the peak amplitude and slope of the AGF function (Figs. 6 and 9) are on average in agreement with results obtained by Ramekers and colleagues in cochlear-implanted guinea pigs (Ramekers et al., 2014). This comparison of findings is further discussed below in section 4.4.

While Ramekers and colleagues (Ramekers et al., 2014) also reported on other ECAP characteristics for which the change in IPG is correlated with neural health in the cochlear implanted guinea pig, some of those measures are not necessarily ideal for use in human subjects. Human subject measurements are limited by sound tolerance levels when measuring ECAPs at higher current stimulus levels. Therefore, measures such as dynamic range of the ECAP AGF (which may be applicable in anesthetized animals) are likely not ideal in human subjects. Further, one ECAP measure that showed a good relationship with the neural health of the animals used in that study was degree to which the current stimulation level corresponding to 50% of the dynamic range along the AGF curve decreased as the IPG was increased. In the current study, we found that this measure becomes difficult to accurately estimate in human subjects because often within the same subject and electrode, increasing the IPG changed the minimum (ECAP threshold) but more importantly the maximum current stimulus levels, thereby changing the dynamic range of the input current stimulus level range and output AGF. For some electrodes (e.g., s99), the shift in current stimulus levels was so dramatic that there was very little overlap in current level values across two IPG conditions, thereby making it difficult or impossible to apply some of the additional measures explored by Ramekers and colleagues. The results reported by Ramekers and colleagues represent data which were collected using identical current stimulation levels with different IPG conditions, and fitted with a sigmoidal equation.

4.4. Relationship with duration of hearing loss

Among the 20 ears evaluated in the current study, the duration of hearing loss prior to implantation spanned a wide range, from approximately 6 years to about 67 years. Given that (1) ECAPs have been shown to reflect neural health in the animals models (Hall, 1990; Prado-Guitierrez et al., 2006; Ramekers et al., 2014; Pfingst et al., 2015) and (2) neural health degrades as a function of duration of hearing loss in humans (Nadol, 1997) it was of interest to examine the extent to which the duration of hearing loss in each ear prior to undergoing implantation could be accounted for by characteristics of the ECAP response. Results showed a significant, negative correlation between ECAP AGF linear slope for a 7 μs IPG and duration of hearing loss (Fig. 11). These results are somewhat in keeping with those reported previously. Brown and colleagues reported significantly steeper AGF slopes in pediatric CI recipients compared to adult recipients (Brown et al., 2010). One could assume that, in most cases, pediatric patients have a shorter duration of hearing loss prior to implantation when compared to their adult peers. In another study, younger adult subjects also had steeper AGF slopes compared to older adult recipients but there was no effect of duration of hearing loss (Cafarelli Dees et al., 2005). It could be argued, however, the duration of hearing loss and/or deafness and subject age can be difficult to parse as they are often correlated with one another. Regardless, the findings in the present study, coupled with those reported previously, argue that suprathreshold measures such as the slope of the AGF are at least partly influenced by characteristics of neural survival and are consistent with findings in cochlear-implanted animals.

No significant relationship was found between duration of hearing loss and the proportional slope change as a function of increasing the IPG from 7 to 30 (Table 4). Recent work in cochlear implanted guinea pigs suggests that the effect of the IPG on suprathreshold ECAP measures is also related to cochlear health (SGN density and perikaryal area) (Prado-Guitierrez et al., 2006; Ramekers et al., 2014). As noted previously, Ramekers and colleagues suggest that larger increases in the proportional ECAP amplitude response as a function of increasing the IPG were negatively correlated with SGN density and perikaryal area. In the same paper, effects of IPG on AGF slopes seem to have an opposite (positive) relationship with cochlear health factors but were not calculated as a proportion. Therefore, as mentioned previously in this manuscript, one might expect a negative correlation for the AGF slope analysis as was observed in the peak amplitude analysis if calculated as a proportion. If so, then we might have expected to find a negative correlation between slope change as a function of increasing the IPG and duration of hearing loss in the current study. However, this relationship was not observed. It is obvious that an estimate of duration of hearing loss in human subjects is not a very precise method to estimate neural health in human subjects. Also, it is important to keep in mind that the mechanism underlying the effect of changing the IPG on suprathreshold ECAP measures is not entirely understood. As mentioned previously, theoretically this measure might reflect aspects of neural health other than density of the stimulated neural population (van den Honert and Mortimer, 1979; Ramekers et al., 2014) which may or may not be related to duration of hearing loss. Further work is needed to better understand effects of IPG manipulation on the ECAP response and what it conveys about specific attributes of cochlear health.

4.5. Summary and future directions

The current study reported on across-site patterns of suprathreshold ECAP measures in 10 bilaterally implanted adults (20 ears). Results showed that patterns of performance varied across subjects, across ears, and were measure dependent. Generally, peak amplitudes and AGF linear slopes were correlated, as were 7 and 30 μs IPG conditions for each ECAP measure. In the present study, we found that increasing the IPG resulted in increased amplitude and slope values. The current study did not focus on across-ear differences in ECAP measures within a subject, as this will be examined in a subsequent study. Additionally, we were unable to precisely assess N1 latency values of ECAP measures in the give study due to the low sampling rate used during data collection. However, given that N1 latency has also been shown to relate to SGN density and it theoretically may be less affected by impedance

factors, this measure could be a plausible choice for clinical application and warrants further investigation in a future study.

The results have implications for how to implement the ECAP measure to maximize CI performance. For example, given that suprathreshold ECAP measures reflect cochlear health in animals, it may be feasible to use these measures to guide the programming of processor maps and improve performance in human CI recipients. Further work is needed to determine how these specific ECAP measures relate to speech recognition. However, these studies do provide evidence that these measures would be useful for diagnosis of individual stimulation sites in a subject's cochlear implant because (a) AGFs were recorded on 89% of the electrodes, and (b) there was significant across-site variability in the ECAP measures even for adjacent sites in some cases. Future work will examine the relationship between these suprathreshold ECAP measures and speech recognition and also use these measures to modify processor maps to improve performance.

Acknowledgements

This work was supported by NIH NIDCD grants R01 DC010786 and P30 DC005188. Portions of this work were presented at The 2016 Mid-Winter Meeting of the Association for Research in Otolaryngology (San Diego, CA), the 2015 Conference on Implantable Auditory Prostheses (Lake Tahoe, CA), and the 2016 Cochlear Implants International Conference (Toronto, ON). We are grateful to the subjects who participated in this study. We thank Monita Chatterjee, Ph.D., and two anonymous reviewers for their reviews of earlier drafts of this manuscript, and Christopher Buswinka for helpful comments regarding the impedance measures. Thanks to the clinicians at the University of Michigan Hearing Rehabilitation Center and the Director of the clinic Teresa A. Zwolan, Ph.D., all of whom assisted with subject recruitment and provided helpful insight on this project.

References

Abbas, P.J., Brown, C.J., Shallop, J.K., Firszt, J.B., Hughes, M.L., Hong, S.H., et al., 1999. Summary of results using the nucleus CI24M implant to record the electrically evoked compound action potential. Ear Hear 20 (1), 45–59.

Abbas, P.J., Hughes, M.L., Brown, C.J., Miller, C.A., South, H., 2004. Channel interaction in cochlear implant users evaluated using the electrically evoked compound action potential. Audiol. Neurootol. 9 (4), 203–213. http://dx.doi.org/10.1159/000078390.

Brill, S., Muller, J., Hagen, R., Moltner, A., Brockmeier, S.J., Stark, T., et al., 2009. Site of cochlear stimulation and its effect on electrically evoked compound action potentials using the MED-EL standard electrode array. Biomed. Eng. Online 8, 40. http://dx.doi.org/10.1186/1475-925x-8-40.

Brown, C.J., Abbas, P.J., Etlert, C.P., O'Brient, S., Oleson, J.J., 2010. Effects of long-term use of a cochlear implant on the electrically evoked compound action potential. J. Am. Acad. Audiol. 21 (1), 5–15.

Brown, C.J., Abbas, P.J., Gantz, B.J., 1998. Preliminary experience with neural response telemetry in the nucleus CI24M cochlear implant. Am. J. Otol. 19 (3), 320–327.

Cafarelli Dees, D., Dillier, N., Lai, W.K., von Wallenberg, E., van Dijk, B., Akdas, F., et al., 2005. Normative findings of electrically evoked compound action potential measurements using the neural response telemetry of the Nucleus CI24M cochlear implant system. Audiol. Neurootol. 10 (2), 105–116. http://dx.doi.org/10.1159/000083366.

Carlyon, R.P., van Wieringen, A., Deeks, J.M., Long, C.J., Lyzenga, J., Wouters, J., 2005. Effect of inter-phase gap on the sensitivity of cochlear implant users to electrical stimulation. Hear Res. 205 (1–2), 210–224. http://dx.doi.org/10.1016/j.heares.2005.03.021.

DeVries, L., Scheperle, R., Bierer, J.A., 2016. Assessing the electrode-neuron interface with the electrically evoked compound action potential, electrode position, and behavioral thresholds. J. Assoc. Res. Otolaryngol. http://dx.doi.org/10.1007/s10162-016-0557-9.

Duan, Y.Y., Clark, G.M., Cowan, R.S., 2004. A study of intra-cochlear electrodes and tissue interface by electrochemical impedance methods in vivo. Biomaterials 25 (17), 3813–3828. http://dx.doi.org/10.1016/j.biomaterials.2003.09.107.

Franks, W., Schenker, I., Schmutz, P., Hierlemann, A., 2005. Impedance characterization and modeling of electrodes for biomedical applications. IEEE Trans. Biomed. Eng. 52 (7), 1295–1302. http://dx.doi.org/10.1109/tbme.2005.847523.

Garadat, S.N., Zwolan, T.A., Pfingst, B.E., 2013. Using temporal modulation sensitivity to select stimulation sites for processor MAPs in cochlear implant listeners. Audiol. Neurootol. 18 (4), 247–260. http://dx.doi.org/10.1159/000351302.

Hall, R.D., 1990. Estimation of surviving spiral ganglion cells in the deaf rat using the electrically evoked auditory brainstem response. Hear Res. 49 (1–3), 155–168.

Holden, L.K., Finley, C.C., Firszt, J.B., Holden, T.A., Brenner, C., Potts, L.G., et al., 2013. Factors affecting open-set word recognition in adults with cochlear implants. Ear Hear 34 (3), 342–360. http://dx.doi.org/10.1097/AUD.0b013e3182741aa7.

Khan, A.M., Handzel, O., Burgess, B.J., Damian, D., Eddington, D.K., Nadol Jr., J.B., 2005. Is word recognition correlated with the number of surviving spiral ganglion cells and electrode insertion depth in human subjects with cochlear implants? Laryngoscope 115 (4), 672–677. http://dx.doi.org/10.1097/01.mlg.0000161335.62139.80.

Long, C.J., Holden, T.A., McClelland, G.H., Parkinson, W.S., Shelton, C., Kelsall, D.C., et al., 2014. Examining the electro-neural interface of cochlear implant users using psychophysics, CT scans, and speech understanding. J. Assoc. Res. Otolaryngol. 15 (2), 293–304. http://dx.doi.org/10.1007/s10162-013-0437-5.

McKay, C.M., Henshall, K.R., 2003. The perceptual effects of interphase gap duration in cochlear implant stimulation. Hear Res. 181 (1–2), 94–99.

Nadol Jr., J.B., 1997. Patterns of neural degeneration in the human cochlea and auditory nerve: implications for cochlear implantation. Otolaryngol. Head. Neck Surg. 117 (3 Pt 1), 220–228.

Nadol Jr., J.B., Shiao, J.Y., Burgess, B.J., Ketten, D.R., Eddington, D.K., Gantz, B.J., et al., 2001. Histopathology of cochlear implants in humans. Ann. Otol. Rhinol. Laryngol. 110 (9), 883–891.

Nehme, A., El Zir, E., Moukarzel, N., Haidar, H., Vanpoucke, F., Arnold, L., 2014. Measures of the electrically evoked compound action potential threshold and slope in HiRes 90K(TM) users. Cochlear Implants Int. 15 (1), 53–60. http://dx.doi.org/10.1179/1754762813y.0000000039.

Pfingst, B. E., Colesa, D. J., Watts, M. M., Su, G. L., Budenz, C. L., & Raphael, Y. (2014). Neurotrophin gene therapy in deafened ears with cochlear implants: long-term effects on nerve survival and functional measures. Paper Presented at the Mid-Winter Meeting of the Association for Research in Otolaryngology, San Diego.

Pfingst, B.E., Zhou, N., Colesa, D.J., Watts, M.M., Strahl, S.B., Garadat, S.N., et al., 2015. Importance of cochlear health for implant function. Hear Res. 322, 77–88. http://dx.doi.org/10.1016/j.heares.2014.09.009.

Polak, M., Hodges, A.V., King, J.E., Balkany, T.J., 2004. Further prospective findings with compound action potentials from Nucleus 24 cochlear implants. Hear Res. 188 (1–2), 104–116. http://dx.doi.org/10.1016/s0378-5955(03)00309-5.

Prado-Guitierrez, P., Fewster, L.M., Heasman, J.M., McKay, C.M., Shepherd, R.K., 2006. Effect of interphase gap and pulse duration on electrically evoked potentials is correlated with auditory nerve survival. Hear Res. 215 (1–2), 47–55. http://dx.doi.org/10.1016/j.heares.2006.03.006.

Ramekers, D., Versnel, H., Strahl, S.B., Smeets, E.M., Klis, S.F., Grolman, W., 2014. Auditory-nerve responses to varied inter-phase gap and phase duration of the electric pulse stimulus as predictors for neuronal degeneration. J. Assoc. Res. Otolaryngol. 15 (2), 187–202. http://dx.doi.org/10.1007/s10162-013-0440-x.

Seyyedi, M., Viana, L.M., Nadol Jr., J.B., 2014. Within-subject comparison of word recognition and spiral ganglion cell count in bilateral cochlear implant recipients. Otol. Neurotol. 35 (8), 1446–1450. http://dx.doi.org/10.1097/mao.0000000000000443.

Shepherd, R.K., Javel, E., 1997. Electrical stimulation of the auditory nerve. I. Correlation of physiological responses with cochlear status. Hear Res. 108 (1–2), 112–144.

Shepherd, R.K., Javel, E., 1999. Electrical stimulation of the auditory nerve: II. Effect of stimulus waveshape on single fibre response properties. Hear Res. 130 (1–2), 171–188.

Smith, L., Simmons, F.B., 1983. Estimating eighth nerve survival by electrical stimulation. Ann. Otol. Rhinol. Laryngol. 92 (1 Pt 1), 19–23.

Stypulkowski, P.H., van den Honert, C., 1984. Physiological properties of the electrically stimulated auditory nerve. I. Compound action potential recordings. Hear Res. 14 (3), 205–223.

Tykocinski, M., Duan, Y., Tabor, B., Cowan, R.S., 2001. Chronic electrical stimulation of the auditory nerve using high surface area (HiQ) platinum electrodes. Hear Res. 159 (1–2), 53–68.

van den Honert, C., Mortimer, J.T., 1979. The response of the myelinated nerve fiber to short duration biphasic stimulating currents. Ann. Biomed. Eng. 7 (2), 117–125.

Zhou, N., Pfingst, B.E., 2014. Effects of site-specific level adjustments on speech recognition with cochlear implants. Ear Hear 35 (1), 30–40. http://dx.doi.org/10.1097/AUD.0b013e31829d15cc.